Optimal Control for Fatigue Reduction of a Ballast-Stabilized Floating Wind Turbine

Department of Electronic Systems

Author:
Giuseppe Battista Abbate

Supervisor:
Professor Jakob Stoustrup
Associate Professor Torben Knudsen

January 2013

AALBORG UNIVERSITY
DENMARK

Table of Contents

Abstract

The increasing demand for renewable energy all the world led to a development in wind power technologies. Thus, wind turbines are increasing in dimension and power production. So far they are mounted on land or in shallow waters with basement. The main disadvantage is that wind turbines have a visual impact that sometimes cannot be accepted. Also, because of the aerodynamic interaction between the wind and the blades, they cause ambient noise near the structure. Hence, the objective during the last years is to install these structures in deeper water, where there's no visual impact and the ambient noise is not relevant. There's also another advantage for going further offshore into deeper waters: wind is less turbulent due to the fact that there are no mountains, buildings or something else that can deviate the wind flow.

The unique economically favourable way to move in deeper water is using floating platform. Fortunately, floating platforms were deeply studied by the oil and gas companies for their oil plants, and these studies have also been used for the wind turbines. However, using a floating wind platform introduces additional motions that must be taken into account in the design stage. Therefore, the control system becomes an important component in controlling these motions. It has been shown that using the onshore baseline controller (PI blade pitch controller plus variable speed generator torque controller) can cause the problem of negative damping in the offshore wind turbine.

The first part of the report aims to describe briefly the tuning procedure of the baseline controller and the development of a simplified control-oriented model of offshore floating wind turbine for a ballast stabilized platform. The analysis focuses on the dynamics of a wind turbine, the development of a model starting from the forces that act on the system, the identification of the parameters and finally the validation of the model using the detailed wind turbine simulator FAST, freely available online and accessible in the literature (1).

The second part of the report describes three types of control techniques for the wind turbines, based on both classic and advanced control theory. It has been used a baseline PI controller and an three LQ controller with different objectives. The purpose is to apply and to analyze a control law that aims to reduce the fatigue in the tower. The main idea was to minimize the variance of the tower deflection or the variance of the tower deflection velocity. The results showed that with the LQ controllers, reducing the tower deflection velocity, it is possible to reduce the fatigue in the tower base.

The last part of the report consists in a comparison between the three LQ controller described before and the baseline PI, based on the Damage Equivalent Loads and on a

statistic analysis. Each controller will be used in simulation with FAST in order to understand if the control law actually minimizes the fatigue and legitimates the use of an advanced controller.

1 Introduction

This chapter briefly describes some statistics about wind power production and an overview of the different types of floating wind turbines and their advantages as well. The state of the art is described, followed by the objective of this project. Finally, an outline of the thesis is described.

1.1 Motivation

Wind power has been used since 5000 B.C. when it was used as propulsion of sailing ship along the Nile river. Later in China, simple windmills were used to pump water, while in the Middle East were used to grind grain. In the Middle Age, windmills were a good integrated part of agricultural processes. In 1887 the first windmill made for electricity production was built by James Blyth in Scotland (2). Anyhow, in the 20^{th} century, coal was cheaper than the electricity generated from wind, so that until fuel prices dramatically rose up in the late 20th century, wind power system's research was not intensificated. Nowadays wind turbines can compete with other sources of energy, and this led to many researches about increasing the power generated by a single wind turbine and the efficiency of the electricity production.

During 2012, 11,895 MW of wind power have been installed across European Union. 10,729 MW of these were onshore and 1,166 MW offshore. Compared with 2011, in 2012 there has been an increase of 51% in terms of wind power plants installed in the EU. Investment for wind farm in EU was between €12.8bn to €17.2bn. Wind power systems were the 26.5% of the new installation in 2012, the second biggest after solar plants. Installations in 2012 were higher than European Wind Energy Association's expectations (3).

Anyway, in different EU countries the growth of big wind farm is obstructed by different factors, among which scarcity of low populated areas and the morphology of the territory.

Under these circumstances, research is now focusing on building wind turbines in harsher environment, such as deeper water with offshore wind turbines. This new technology can provide at least four advantages (4):

- Large areas are available for wind farm development with limited environmental impact
- Mean wind speeds are high and this leads to higher energy production
- Wind turbulence is lower than in the onshore wind turbines

- There’s no limitation about the dimensions of the wind turbines caused by their visual impact and/or noise

However, there are economic disadvantage for installing wind turbines offshore, such as higher capital and operating costs (5).

Different kind of offshore wind turbines have been used, depending on water depth.

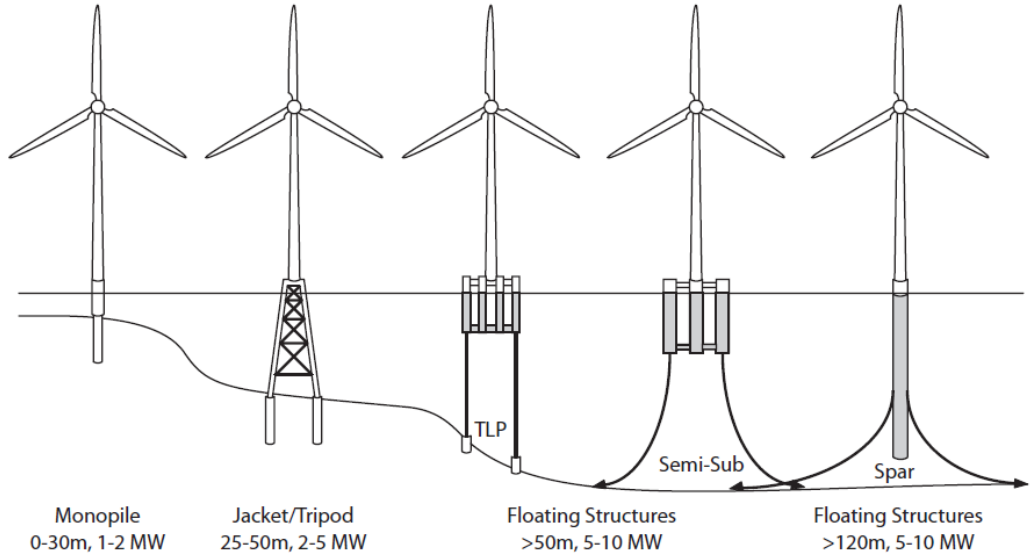

Figure 1.1 – Different types of offshore wind turbines (6)

Basically, it is cheaper to use foundations in water depth until 50 m, where installation costs are sufficiently low. For deeper water using floating platforms is preferable, anchoring them to the seabed by mooring lines, as presented in Figure 1.1. Nowadays the most promising technologies for the offshore platforms are the ballast stabilized platform and the tension leg (7):

- Stabilization in the spar buoy platform is guaranteed by a considerable mass placed at the bottom of the floating platform, that is usually at a very high depth. This mass avoid the capsizing of the structure moving the position of the center of mass, that is always deeper than the center of buoyancy.
- In the TLP the structure has a buoyancy force higher than the weight force of the whole structure. This platform is kept under the SWL by tie-rods planted on the seabed at high tension.

In (8) a comparison between the different platform structures is presented, based on the performances and costs. It is shown that the ballast stabilized has an advantage regarding construction costs of platform and mooring lines, thanks to its simplicity. Waves have also lower impact on the ballast stabilized, thanks to its small surface in contact with them. Anyhow, both of them increase the motion of the wind turbine, that is subject to hydrodynamic loads in addition to the aerodynamic loads to which an onshore wind turbine is normally ruled. These dynamics lead to lower natural frequency of the structure: the baseline PI controller used in the onshore wind turbine cannot therefore be used in the offshore wind plant with no alterations, because it would excite the structure and cause damage and/or higher fatigue. Therefore, it is

necessary to include a logic in the controller allowing the higher possible increase of the lifetime of the offshore wind turbine.

Objectives

In (9) an LQ controller for a ballast stabilized offshore wind turbine has been developed. It was showed that an optimal control could reach greater performance compared to the detuned PI controller described in (10). The results showed that it was possible to have a decrement of variation of the generated power and of the tower loads.

Figure 1.2 - The Hywind Demo: 2.3 MW Siemens Wind Turbine mounted on a ballast stabilized platform

The main objective of the new control law was to reduce the tower deflection with respect to the platform. To address this objective a variation has been made in the model described by Christiansen, including two different degrees of freedom for the platform and the tower. Methods of system identification have been used to find the parameters of this model, and the linear quadratic optimal controller has been applied with the specific objective of reducing the difference between the motion induced by the tower and the one induced by the platform. Simulations are made by means of FAST (1), a free code developed by NREL capable to simulate the aerodynamics and hydrodynamics of a wind turbine with high fidelity. The results are finally evaluated by means of statistic methods and the study of the damage equivalent loads (DEL).

In the following report only the ballast stabilized offshore wind turbine has been considered, referring to the Hywind project developed by Statoil (11). This is the first world full-scale floating wind turbine, sited ten kilometers off the south of Norway. In this dissertation a sort of standardized version of Hywind is considered, adapted for simulation with FAST.

1.2 State of the Art and Background

Since the second part of last decade floating wind turbines are an interesting field of research. To evaluate the actual background on floating wind turbines, state of the art of modeling and control methods will be presented.

A high fidelity simulation code is described in (12) and (13): in these a coupled hydro and aero dynamic model for describing the behavior of an offshore floating wind turbine is presented.

In (14) a preliminary down-scaled model of the Hywind Demo has been presented. The purpose of this research was to describe and to compare two different simulation programs for integrated dynamic analysis of floating wind turbines with the down-scaled model of the Hywind at different condition. The results showed that both the simulations agreed with the experiment made.

An analysis about the pitch control impact on the fatigue has been made in (15), where a method to compute fatigue damages is presented. The results showed that the fatigue damages of the tower and rotor depend both on environmental conditions and on pitch control strategy.

The problem of the negative damping is addressed in (16). The negative damping is a phenomenon that can be seen when a baseline controller tuned for the onshore wind turbine is mounted on an offshore wind turbine. When in an onshore wind turbine the wind pushes the tower backward, the controller decreases the blade pitch angle because the relative wind speed is decreased. Thus, the thrust force increases. Conversely, if the tower is moving forward, the controller acts to increase the blade pitch angle, so the thrust force is reduced. This behavior in an onshore wind turbine is not problematic but due to the higher number of DOFs of the floating wind turbine, can cause big oscillations that turn in reduced lifetime of the structure. Larsen and Hanson in their work found that the lowest natural frequency of the floating structure is lower than the frequency used for the onshore controller. Thus, they suggested to detune the baseline controller to provide stable tower vibration modes. At cost of worst performance in power generation, the system showed stability.

In (17) three tentative to adapt the baseline controller for a wind turbine mounted on a ITI Barge are presented. Jonkman added a feedback of the tower top acceleration to the baseline controller, an active pitch-to-stall (instead of the most used pitch-to-feather) and the detuning of the baseline controller. Only the third approach showed to improve the platform pitch response.

The use of an optimal controller is analyzed in (18). A model considering both platform pitch and rotor azimuth DOFs is developed and used for generate an LQ controller. Namik and Stol also applied an individual blade pitch control law. The results showed that the LQR collective blade pitch controller could increase the performance in terms of rotor speed regulation and platform pitch regulation. This result anyway has to be addressed to the use of constant torque control for the generator, instead of constant power. The individual blade pitch control showed to

improve the performance of the LQR controller, but it added a rolling moment that could destabilize the system.

Another variation of the baseline PI controller is addressed in (19). In order to maintain the control structure generally preferred by wind turbine manufacturers such as a PID, the idea was to change the set point of the generator speed depending on the platform pitch motion. When the platform is pitching forward the generator speed set point is set to a larger value, so that the PID regulator will decrease the blade pitch angle, hence the thrust force will increase and the wind turbine will move to the upright position. Lackner also developed another individual blade pitch controller based on Namik's work, but with the specific object to reduce loads on the blades. Results showed that with the first approach it is possible to reach reduced motion of the platform, increasing insignificantly the generator speed variation. The blade loads were reduced too, but still higher compared to the onshore case. The IBP instead appeared to be negligibly effective on the floating case.

In (20) two individual blade pitch approaches were discussed. The first used a 6 DOFs model coupled with a LQ controller, the second added a disturbance accommodating control, where the disturbances were wind and waves. The work showed a considerable increasing in the generator speed regulation without severely affecting other main turbine components for the first control. The DAC instead presented just a negligible improvement compared to the IBP with 6 DOFs.

Jonkman, in (10), defined the structure of a 5 MW wind turbine based on the Hywind Demo project. Also, the baseline controller of a ballast stabilized wind turbine is defined. In this report it is suggested to use a constant torque control for the generator to avoid the negative damping in the Hywind.

In (9) an optimal control based on a linear quadratic regulator was applied. The model is made including drivetrain flexibilities and platform motion. It was also considered an observer for estimating the state of the model. Wind was estimated by means of an Extended Kalman Filter, considering the wind turbulence as a second order system. Results were compared to the baseline controller and presented an improvement in the generator speed regulation and a reduction in the fatigue loads. This is the work on which the following dissertation is based on. The model is upgraded with another DOF so as to describe the motion of the platform and of the tower.

In (21) an optimal control strategy is presented based on the minimum thrust using a variable generator torque above rated condition. The results showed that this strategy can reduce oscillations of both tower and platform, at cost of an increased blade pitch activity and drivetrain torsion.

Another work of Christiansen addressed the influence that wave frequency and misalignment between wind and wave direction have on the wind turbine dynamics (22). A control oriented model has also been developed, in which are considered additional platform DOFs, the mooring system and the side side motion of the tower. An estimator of wind speed and wave frequency are then included. Improvement in

generator speed regulation, platform pitch and tower deflection. The possibility to use the induced generator torque has been introduced to damp the side side motion of the tower and the platform roll.

In (23) a specific model for the spar buoy platform is developed. An H_∞ control strategy has also been applied. The simplified 2D model simulations appeared to be very close to the ones made by FAST when the H_∞ control is applied.

2 Methods

In order to transform the kinetic energy of the wind in electric power, wind turbines need different kind of mechanic and electric components. In this dissertation the behavior of the electronic system needed for the conversion of mechanical power to electric power will not be discussed. The focus is on the mechanic structures of the wind turbines, and the way they are controlled. The main important component of an aerogenerator are the following:

- Tower
- Nacelle
- Hub and blades
- Drivetrain
- Generator

At the top of the tower the nacelle and the hub are mounted. The hub is connected to the blades and to a gearbox by the drivetrain. Finally, the gearbox is connected to the generator.

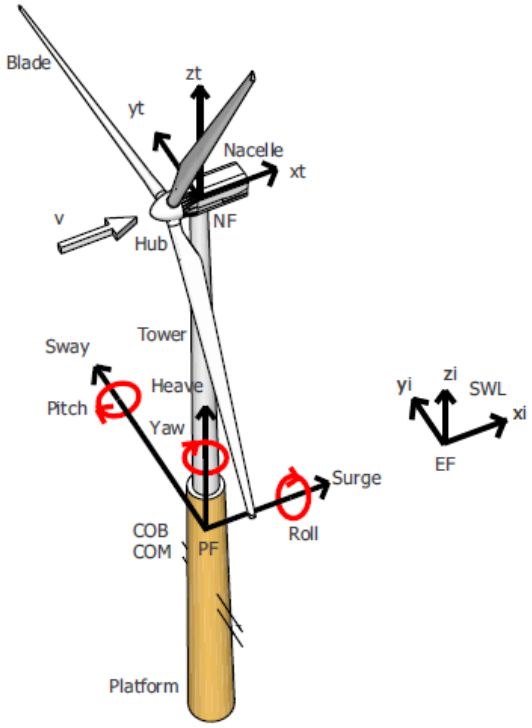

Figure 2.1 – Floating three bladed wind turbine mounted on a spar buoy platform (6)

The electric power is the output of a wind turbine, and the main objective of a wind turbine is to maintain it as constant as possible. The output is given by:

$$P_e = \omega M_g \quad (2.1)$$

where ω is the generator speed and M_g is the induced generator torque. Both the generator speed and the generator torque can be controlled. The generator speed is dependent by the relative wind speed. As long as the rotor is subjected to a sufficient wind, an aerodynamic torque is applied to it, causing a rotation of the rotor. This rotation is then transferred to the gearbox and finally to the generator. Inducing an opposite torque on the generator makes it possible to produce electric power from the wind. This mechanism is relatively complicated, and needs the use of non linear equations to describe at its best the behavior of the complete system. Anyway, it is possible to describe it by means of linear equations around a certain operating point. This is an approximation of the real trajectories of the dynamic system, but it can be considered sufficient for the purposes of this thesis.

In an onshore wind turbine different degrees of freedom (DOF) act on the structure. First of all the rotor is able to rotate around the x_t axis. The drivetrain is subjected to torsion, due to the fact that the rotor speed and the generator speed are not always equal. The tower is subjected to deflection, that can be described by the motion of the tower top. There are two main deflection of the tower: fore-aft, directed on the x_t axis, and side-side, directed on the y_t axis. Finally, the blades are usually deflected. Their deflection can be edgewise or flapwise.

In a floating wind turbine (FWT) such as the Hywind Demo there are six degree of freedom more than in the onshore wind turbines. The presence of the platform in fact causes additional motions of the complete wind turbine. The tower base can translate and rotate, on the three axis x_i, y_i, z_i.

2.1 Wind Turbine Dynamics

The interaction between the different component of a floating wind turbine can be successfully described by the Figure 2.2 – Scheme of the coupled dynamics of a wind turbine :

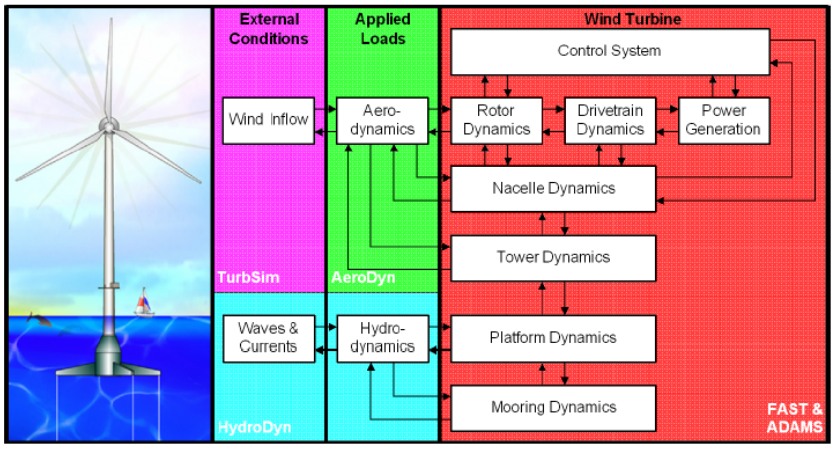

Figure 2.2 – Scheme of the coupled dynamics of a wind turbine (13)

The control system acts on the rotor dynamics and on the power generation changing the rotor speed and the induced generator torque. The rotor and the drivetrain are then connected to the structure, composed by the nacelle, the tower, the platform and the mooring lines. The interaction between the wind turbine and the ambient condition are described by the aerodynamics and the hydrodynamics.

Aerodynamics

The wind acts on the rotor generating an aerodynamic torque and thrust. Both of them depends on the tip speed ratio λ, the rotor speed Ω, the relative wind speed v_r, the blade pitch angle β and the intrinsic characteristic of the wind turbine and the environment (5):

$$M_a = \frac{1}{2}\frac{1}{\Omega}\rho A C_p(\lambda,\beta)v_r^3 \quad (2.2)$$

$$F_a = \frac{1}{2}\rho A C_t(\lambda,\beta)v_r^2 \quad (2.3)$$

where the TSR is defined as:

$$\lambda = \frac{\Omega R}{v_r} \quad (2.4)$$

The above equation are strongly nonlinear, but they can be linearized and used in a model-based control. Note that, in the FWT, the relative wind speed is very important in the dynamics of the system, due to the added motion of the platform.

Hydrodynamics

In the model used in this thesis the problem of the interaction between the waves and the platform is not addressed. The impact that the water has on the platform is mainly described by the hydrostatic forces, that are the buoyancy and the gravitational forces. The buoyancy force is dependent from the displaced volume submerged, while the gravitational force is dependent from the mass of the wind turbine.

2.2 Fatigue in a Wind Turbine

A typical wind turbine is subjected to severe fatigue loadings in its lifetime. Hence a wind turbine, after a certain number of rotation of the rotor or oscillation of the tower, can be affected by severe damage or permanent deflection. The design of the components and the control is often governed by fatigue than extreme loads. This is because a wind turbine is an investment, and to be economically feasible must guarantee a certain lifetime: if the components last less than the desired lifetime, the investment is not lucrative. Thus, a controller designer must take into account also the fatigue of the wind turbine, and not only the performances of the electric power in output. The purpose of this dissertation is to reduce the fatigue in the tower for the Hywind wind turbine. In order to do so it is important to identify a model for the fatigue, that will be used to find the control objectives of the LQ.

For each material can be identified a critical level of fatigue, over which it breaks or it has permanent deformation. This level can be described by means of a stress curve

over the number of cycles, as showed in Figure 2.3 – Stress vs Number of cycles curve for a generic material.

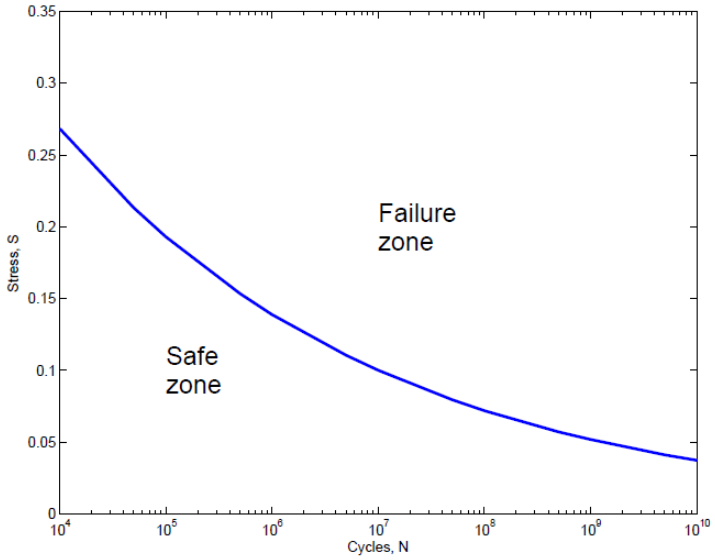

Figure 2.3 – Stress vs Number of cycles curve for a generic material (6)

Under the blue line the stress is lower than its critical value, so the component will not have any severe damage. The opposite is true in the failure zone. The curve is well approximated by equation (2.5):

$$S = K\,N^{-\frac{1}{k}} \qquad (2.5)$$

where S is the stress level, N is the number of cycles and k is the Wöhler coefficient. Anyhow, this approach cannot be used for continuous time system, where it is preferred to use the rainflow counting (24). The rainflow counting is an application of the Miner's rule that states that if there are k different stress levels S_i in a spectrum, each contributing with $n_i(S_i)$ cycles, then if $N_i(S_i)$ is the number of cycles to failure, the damage is:

$$D = \sum_{i=1}^{k} \frac{n_i}{N_i} \qquad (2.6)$$

D is experimentally found to be between 0.7 and 2.2, and represents the actual damage level with respect to the critical damage.

In this thesis, in order to compare the results of the different controllers Damage Equivalent Loads (DEL) are used. The most important DELs, that will be used in this dissertation, are the ones of the tower, blade edgewise and flapwise and of the drivetrain. While the tower base loads and the blade root loads can be considered a direct measure of the fatigue in the structure, the LSS torque has been chosen for the drivetrain DEL, because directly available as an output in FAST. Besides, using a constant torque approach, the low speed shaft torque is able to represent the torsion loads acting on the drivetrain, and then its fatigue. Comparing these DELs and the standard deviation of the electric power is possible to understand which of the controllers is the best to reduce the fatigue in the tower.

2.3 Control Structure in Wind Turbines

A wind turbine consists of sensors, actuators and a control system that uses both of them to maintain high efficiency of the wind turbine and safe turbine operation. Also, the controller tries to reduce the damage fatigue loads and to detect fault conditions (25).

Variable-Speed Turbine Operating Regions

Typical variable-speed wind turbines have different regions of operation. These regions are defined by the generator speed, relatively easy to measure at the HSS in a real wind turbine. For each region an optimal generator torque is defined. A very common curve used for the variable speed generator control is presented in Figure 2.4:

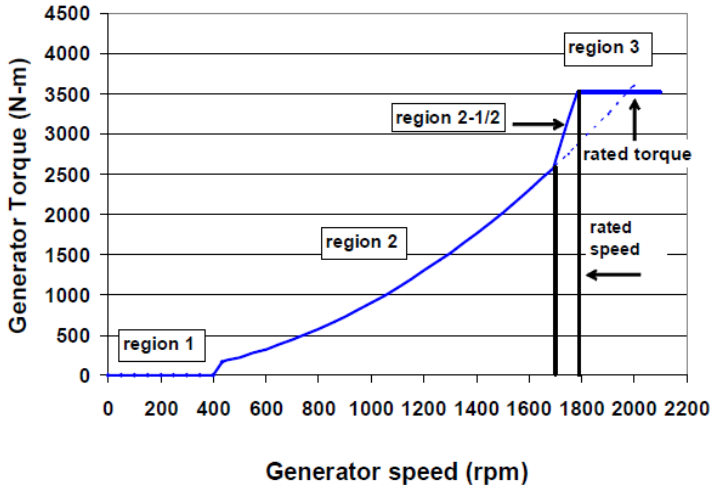

Figure 2.4 – Generator Torque over Generator Speed curve in a baseline variable speed control (25)

Region 1, or "start-up", occurs for low generator speed. In this region the generator torque is set to zero, because wind is too slow to produce energy. The blade pitch angle is set to stall, therefore the rotor does not move. In region 2, or "partial-load", the generator torque follows an optimal C_p curve, so as to have the best energy capture. The generator torque is used to vary the generator speed, in order to maintain the TSR on its optimum. The blade pitch angle in this region is set to feather. The optimum C_p curve intersects the rated generator torque at a high generator speed, so it is necessary a transitional linear region, called Region $2\,1/2$. At rated generator speed, it is applied the rated torque. In Region 3, or "full-load", a constant power (torque depend on the inverse of generator speed) or a constant torque approach can be applied. In this region the pitch control takes place to the generator speed controller. The objective is to maintain the generator speed as constant as possible, avoiding to excite the structure of the wind turbine.

2.4 Region 3 Control

In this thesis the control in full-load region will be addressed. In order to obtain a comparison of the performances, four different controllers are described: a baseline PI controller and three LQ regulators based on a nine state model with different objectives.

2.4.1 Baseline Controller

This section will briefly describe the tuning procedure of a gain-scheduled proportional integral (PI) control on the error between the measured generator speed and the rated generator speed (26). In order to design the blade pitch controller a single DOF model of the wind turbine is considered. The DOF is the angular rotation of the low speed shaft. Considering a simple free-body diagram of the drivetrain as in Figure 2.5:

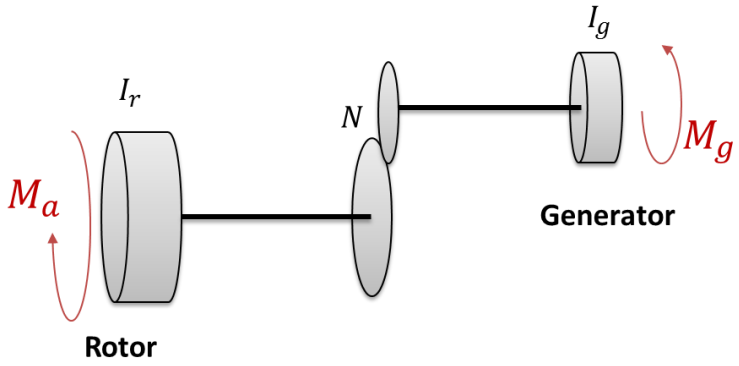

Figure 2.5- Simple free-body diagram of a rigid drivetrain used for the PI tuning procedure

The equation of motion is:

$$M_a - N \cdot M_g = (I_r + N^2 I_g)\Delta\dot{\Omega} \qquad (2.7)$$

where M_a is the aerodynamic torque, M_g is the induced generator torque and Ω is the rotor speed. Linearizing M_a with respect to the rotor speed and the blade pitch angle β, substituting β with the PI control law of the equation (2.8):

$$\beta = K_p \, \mathrm{N} \, \Delta\Omega + K_I \int N \, \Delta\Omega \, dt \qquad (2.8)$$

the equation (2.7) can be seen in the classic second-order model form:

$$M \, \ddot{\Omega} + D\dot{\Omega} + K\Omega = 0 \qquad (2.9)$$

It is now possible to choose the natural frequency and the damping ratio by changing the K_p and K_I gains as follows:

$$\omega_n = \sqrt{\frac{K}{M}} \qquad \zeta = \frac{C}{2 \, M \, \omega_n} \qquad (2.10)$$

These two parameters depend by the derivative of the generated power with respect to the blade pitch angle. This derivative varies considerably over the full load region. Thus, it is suggested to use a gain scheduled controller, that can be obtained

multiplying the K_p and K_I gains by a function $GK(\beta)$ dependent by the blade pitch angle:

$$GK(\beta) = \frac{1}{1 + \frac{\beta}{\beta_k}} \qquad (2.11)$$

where β_k is the blade pitch angle where the derivative of the power has doubled its value at rated operating condition.

According to (16), the controller frequency should be lower than the smallest natural frequency of the structure, that in case of a FWT is near to 0.22 rad/sec (induced by the platform). Hence, reasonable values for the closed loop frequency and damping are:

$\omega_n = 0.2\, rad/sec \qquad \zeta = 0.7$

It has also been added a blade pitch and blade pitch rate saturation, including an anti-windup scheme. The blade pitch actuator is considered to be a low pass filter with a reasonable time constant.

2.4.2 LQ

In order to apply an optimal LQ controller it is necessary to develop a linear model of the main dynamics of the floating wind turbine. In the following model the drivetrain torsion, the tower flexibility, the platform motion, the blade pitch actuator and the wind dynamics are considered.

2.4.2.1 Model

Drivetrain

The drivetrain is modeled as two inertias connected by an ideal torsional spring and damper and a gearbox. Considering the system in the Figure 2.6 it is possible to write the equation using the rotor speed Ω, the generator speed ω and the twist angle ϕ:

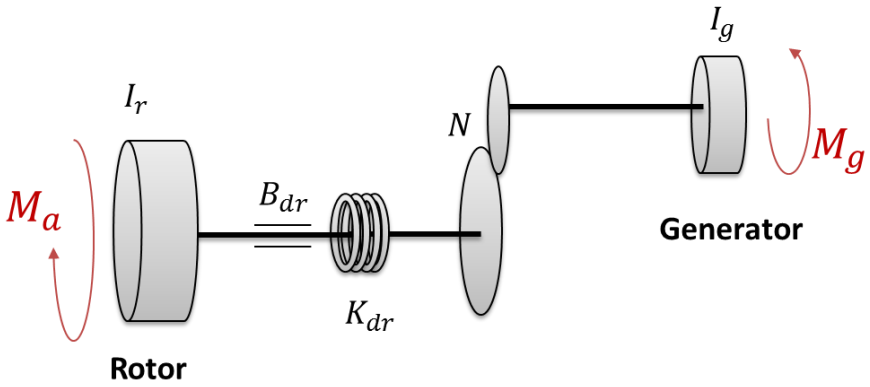

Figure 2.6 – Diagram of the flexible drivetrain used in the LQ9 model

The model will be described by the second order system of the equation (2.12):

$$\begin{cases} \dot{\Omega} = -\frac{B_{dr}}{I_r}\Omega + \frac{B_{dr}}{NI_g}\omega - \frac{K_{dr}}{I_r}\phi + \frac{1}{I_r}\mathrm{M_a} \\ \dot{\phi} = \Omega - \frac{1}{N}\omega \\ \dot{\omega} = \frac{B_{dr}}{NI_g}\Omega - \frac{B_{dr}}{N^2 I_g}\omega + \frac{K_{dr}}{NI_g}\phi + \frac{1}{I_g}\mathrm{M_g} \end{cases} \quad (2.12)$$

where I_r and I_g are the rotor and generator inertias, N is the gear ratio and K_{dr} and B_{dr} are the equivalent spring and damper coefficient of the drivetrain.

Tower and Platform

The model does not include the translation of the platform for simplicity reasons. This can be considered an extreme simplification, but in this thesis the purpose is to define an LQ objective that can reduce the tower fatigue: the results can be easily upgraded including in the model the translation of the platform. The tower and the platform are modeled as two rigid bodies connected by a spring and damper, as presented in Figure 2.7. Two different DOFs are considered in order to describe the motion. The first, γ, is the angle of the tower with respect to the vertical and undeflected position, while α is the angle between the platform and the vertical position.

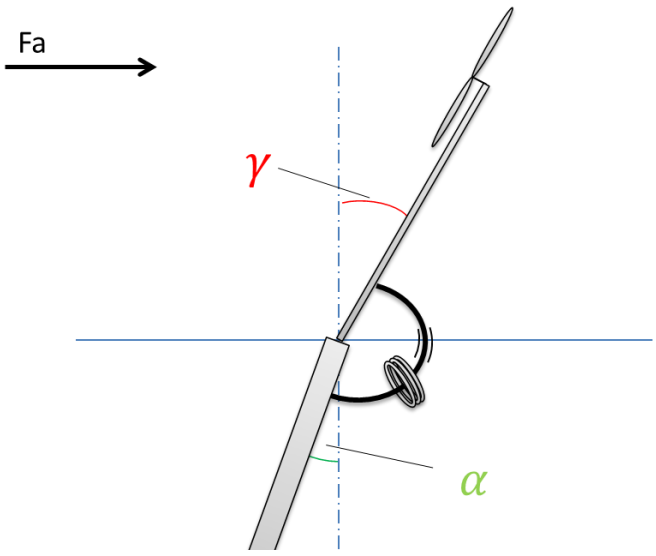

Figure 2.7 – Body diagram of the model used for the platform and the tower: γ and α are the angles of the tower and platform with respect to the vertical and undeflected position of the wind turbine. The two bodies are connected by a spring and a damper.

The difference between γ and α specifies the tower deflection, that is actually what will be considered in two LQ controllers. The equations for this model are illustrated by means of an equilibrium of the moments acting on the tower and the platform.

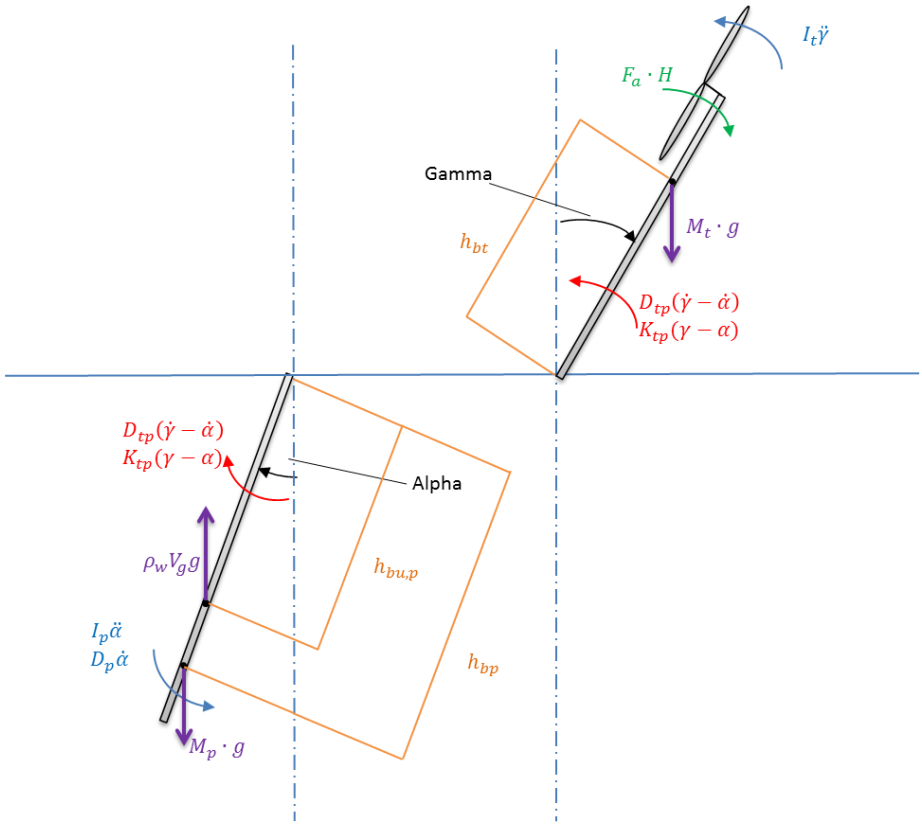

Figure 2.8 – Scheme of the moments and forces acting on the tower and on the platform.

In Figure 2.8 the gravity forces are represented, where M_t and M_p are respectively the masses of the tower and the platform, the buoyancy force, given by the displaced volume V_g and the water density ρ_w, and the thrust moment induced by the wind on the tower. The coefficients D_{tp} and K_{tp} describe the connection between the tower and the platform. I_t and I_p are the inertia of the tower and the platform over the intersection between the SWL and the vertical position of the wind turbine. D_p models the interaction between the water and the platform. In the Equation (2.13) the model is written:

$$\begin{cases} I_t\,\ddot{\gamma} = M_t g h_{bt}\sin(\gamma) + F_a H - D_{tp}(\dot{\gamma} - \dot{\alpha}) - K_{tp}(\gamma - \alpha) \\ I_p\ddot{\alpha} + D_p\dot{\alpha} = \rho_w V_g g h_{bu,p}\sin(\alpha) - M_p g h_{bp}\sin(\alpha) + D_{tp}(\dot{\gamma} - \dot{\alpha}) + K_{tp}(\gamma - \alpha) \end{cases} \quad (2.13)$$

where h_{bt} and h_{bp} represents the application point of the tower and platform gravity force, $h_{bu,p}$ is where the buoyancy force is applied and H is the height of the tower.

Actuator and Wind

The blade pitch actuator β is modeled as a low pass filter. The equation is then:

$$\dot{\beta} = \frac{1}{\tau_\beta}(\beta_c - \beta) \quad (2.14)$$

where β_c is the input of the system. The wind v_t is considered as constant:

$$\dot{v_t} = 0 \quad (2.15)$$

Aerodynamic Torque and Thrust

As previously described, M_a and F_a are nonlinear and depending on the TSR λ and the blade pitch angle β as presented in equations (2.16):

$$M_a = \frac{1}{2}\frac{1}{\Omega}\rho A C_p(\lambda,\beta)v_r^3$$
$$F_a = \frac{1}{2}\rho A C_t(\lambda,\beta)v_r^2 \qquad (2.16)$$
$$\lambda = \frac{R\Omega}{v_r}$$

In this model the relative wind speed v_r is given by:

$$v_r = v_t - \dot{z} \qquad (2.17)$$

In order to have a linear model it is necessary to develop a first order Taylor approximation around an operating point. The chosen operating point is in Region 3:

$$\begin{cases}\Omega_{zero} = 12.1\ rpm \\ v_{r,zero} = 18\ m/s\end{cases}$$

2.4.2.2 Parameters and Identification

The model used for the drivetrain is the same used in (26). The parameters can be easily found in his work. In the Table 2.1 the parameters for the drivetrain are presented:

Parameter	Value
Kdr	8.676E+08 Nm/rad
Bdr	6.215E+06 Nm/(rad/s)
N	97
Ir	3.875E+07 Kg m^2
Ig	5.341E+05 Kg m^2

Table 2.1 – Parameters of the flexible model of the drivetrain

As time constant of the blade pitch actuator is used a reasonable value of $\tau_\beta = 0.2$ seconds.

In order to apply the MATLAB function $lqr()$ the wind dynamic is changed using:

$$\dot{v_t} = -10^{-1.5}\, v_t \qquad (2.18)$$

Derivatives of C_p and C_t

The derivatives of the M_a and F_a used in the state space equation can be computed from the derivative of C_p and C_t with respect to the TSR and the blade pitch angle. From a data-sheet of these coefficients tabulated for different λ and β the derivatives of C_p are computed by means of perturbation of the TSR maintaining a constant β near the operating point, and vice versa:

$$\frac{dC_p}{d\lambda} = \frac{C_p(eq)-C_p(pert)}{\lambda(eq)-\lambda(pert)} \qquad \frac{dC_p}{d\beta} = \frac{C_p(eq)-C_p(pert)}{\beta(eq)-\beta(pert)} \qquad (2.19)$$

The same is done for the thrust coefficient.

Tower Top Identification

In order to use an identification procedure, the equation (2.13) has been modified. Linearizing the $\sin(\delta) \simeq \delta$ and the F_a it is possible to re-order the equations as follows:

$$\begin{cases} M_t\,\ddot{\gamma} + D_t\dot{\gamma} + K_t\gamma = \dfrac{dFa}{d\Omega}H\,\delta\Omega + \dfrac{dFa}{d\beta}H\delta\beta + \dfrac{dFa}{dV_t}H\,\delta V_t - D_{tp}(\dot{\gamma} - \dot{\alpha}) - K_{tp}(\gamma - \alpha) \\ I_p\ddot{\alpha} + D_p\dot{\alpha} + K_p\alpha = D_{tp}(\dot{\gamma} - \dot{\alpha}) + K_{tp}(\gamma - \alpha) \end{cases} \quad (2.20)$$

The parameters to identify are then:

$$\{I_t, D_t, K_t; I_p, D_p, K_p; D_{tp}, K_{tp}\}$$

The identification is developed by means of a step response from FAST, made imposing oscillations in the tower changing the blade pitch angle. The step response is made at 18 m/s constant wind speed, changing the blade pitch angle from 14.92 deg to 15.2 deg, so as to be sure that the operating point is in Region 3.

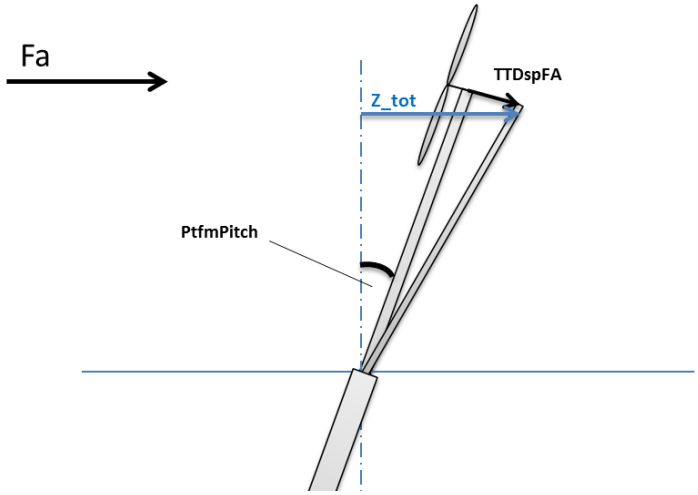

Figure 2.9 – TTDspFA and PtfmPitch are the available output in FAST. The total displacement z_{tot} is given by the sum of these two contribute.

In FAST the available output are the tower top deflection with respect to the undeflected position (TTDspFA), and the platform pitch angle (PtfmPitch). Thus, the total tower top displacement is given by the equation (2.21):

$$z_{tot} = TTDspFA \cdot \cos(PtfmPitch) + H \cdot \sin(PtfmPitch) \quad (2.21)$$

where H is the tower height. The effect of the platform pitch is dominant, as it is possible to see from the Figure 2.10:

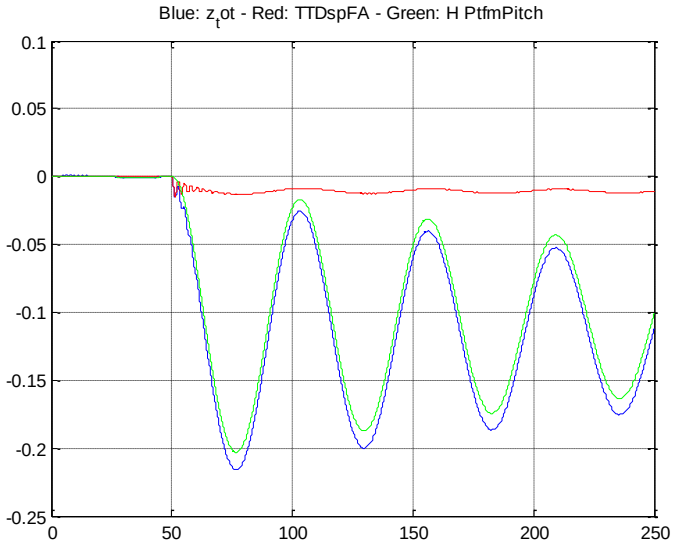

Figure 2.10 – Contributions of the platform pitch (green) and tower deflection (red) to the total tower top displacement (blue) in a blade pitch step in open loop.

Starting from the above step response it has been used the "Control and Estimation Tool Manager". Implementing the equation (2.20) in Simulink is possible to identify the parameters. The identification procedure showed good matching between the measured and the linear step response.

In order to validate the identification an open loop simulation of the linear system has been made including the dynamics of the drivetrain, the tower and the platform compared to a FAST simulation, that is the state space representation of the equation (2.23) . A step in both blade pitch angle and wind speed are made. The results for a wind speed step from 18 m/s to 19 m/s are showed in Figure 2.11, Figure 2.12 and Figure 2.13:

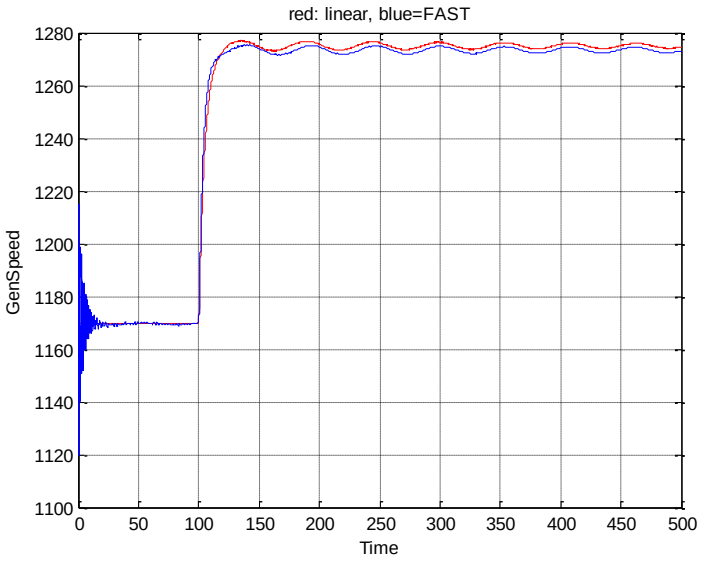

Figure 2.11 – Generator speed response of a wind speed step in FAST and with the linear model.

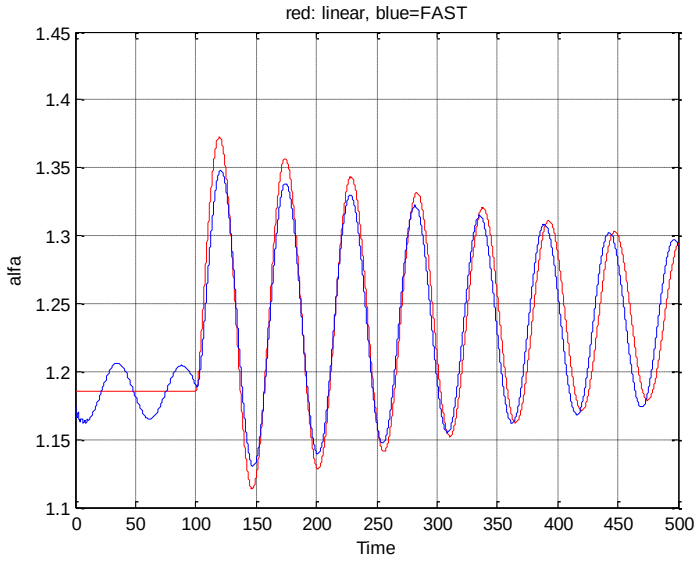

Figure 2.12 – α (angle of the platform) response of a wind speed step in FAST and with the linear model.

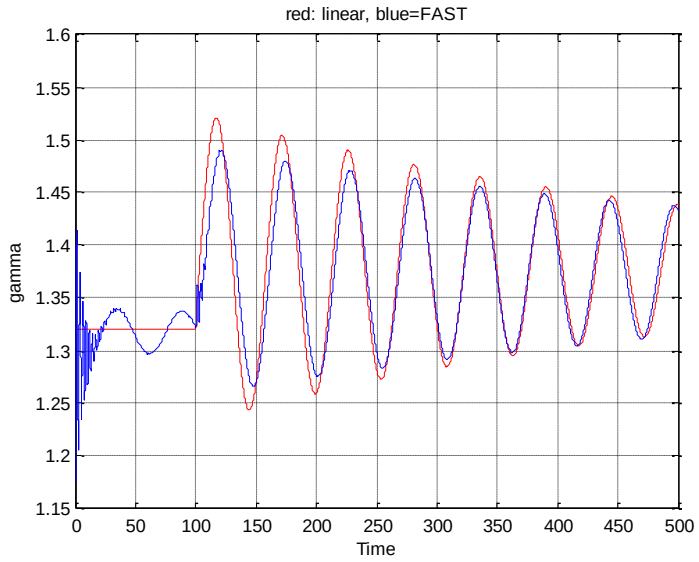

Figure 2.13 – γ (angle of the tower) response of a wind speed step in FAST and with the linear model.

The results showed a good matching in the generator speed, and an acceptable behavior in γ and α. Note that the first 30 seconds of the simulation are not representative of the real behavior of the system.

State Space Model

Starting from the previous equations it is possible to write the state space model. The state vector has seven elements, while the control input is a scalar:

$$x = \{\Omega\ \phi\ \omega\ \alpha\ \gamma\ \dot{\alpha}\ \dot{\gamma}\ \beta\ v_t\}^T \qquad u = \beta_c$$

Considering the state space model described in the equation (2.22):

$$\begin{cases} \dot{x} = Ax + Bu \\ y = Cx + Du \end{cases} \qquad \textbf{(2.22)}$$

The A, B, C and D matrixes are:

$$A = \begin{vmatrix} \frac{-B_{dr} + \frac{dMa}{d\Omega}}{I_r} & -\frac{K_{dr}}{I_r} & \frac{B_{dr}}{I_r N} & 0 & 0 & 0 & \frac{\frac{dMa}{d\dot{z}} * H * \frac{pi}{180}}{Ir} & \frac{\frac{dMa}{d\beta}}{Ir} & \frac{\frac{dMa}{dv_t}}{Ir} \\ 1 & 0 & -\frac{1}{N} & 0 & 0 & 0 & 0 & 0 & 0 \\ \frac{B_{dr}}{I_g N} & \frac{K_{dr}}{I_g N} & -\frac{B_{dr}}{I_g N^2} & 0 & 0 & 0 & 0 & 0 & 0 \\ 0 & 0 & 0 & 0 & 0 & 1 & 0 & 0 & 0 \\ 0 & 0 & 0 & 0 & 0 & 0 & 1 & 0 & 0 \\ 0 & 0 & 0 & \frac{-K_p - K_{tp}}{I_p} & \frac{K_{tp}}{I_p} & \frac{-D_p - D_{tp}}{I_p} & \frac{D_{tp}}{I_p} & 0 & 0 \\ \frac{\frac{dFa}{d\Omega} H}{I_t} & 0 & 0 & \frac{K_{tp}}{I_t} & \frac{-K_t - K_{tp}}{I_t} & \frac{D_{tp}}{I_t} & \frac{-D_t - D_{tp}}{I_t} & \frac{\frac{dFa}{d\beta} H}{I_t} & \frac{\frac{dFa}{dv_t} H}{I_t} \\ 0 & 0 & 0 & 0 & 0 & 0 & 0 & -\frac{1}{\tau_\beta} & 0 \\ 0 & 0 & 0 & 0 & 0 & 0 & 0 & 0 & -10^{-1.5} \end{vmatrix}$$

(2.23)

$$B = \begin{vmatrix} 0 \\ 0 \\ 0 \\ 0 \\ 0 \\ -\frac{1}{\tau_\beta} \\ 0 \end{vmatrix} \qquad C = \begin{vmatrix} 0 & 0 & 1 & 0 & 0 & 0 & 0 \\ 0 & 0 & 0 & 0 & H & 0 & 0 \end{vmatrix} \qquad D = 0$$

The system presents a coupling effect between the generator speed and the tower displacement, as can be seen by the terms $\frac{dMa}{d\dot{z}}$ and $\frac{dFa}{d\Omega}$ in the matrix A. Both the generator speed and the tower top displacement are considered as a measure. Without the measure of the tower top displacement in fact the system is weakly observable, and causes a decline of the control. Anyhow, the displacement can be computed by a double integration of the measure of an accelerometer. This is not very used in industry, due to the noisy measure made for the tower top acceleration, but it shouldn't affect the results of the thesis.

2.4.2.3 Linear Quadratic Regulator

The LQ controller for a wind turbine is well described in the Appendix A. In this part the control objectives and the choices made for the matrixes Q, R and N will be described. Three different control objectives will be discussed.

Kalman Filter

In order to use an LQ controller a Kalman filter has been chosen to estimate the states of the system starting from the available measures. Better understanding of the implementation of the Kalman filter for a wind turbine can be found in the Appendix A. Here the Q and R matrixes used will be explained.

The weight matrixes for the observer are defined as identity matrix of the correct dimension for both.

$$Q_{obs} = eye(9) \qquad R_{obs} = eye(2)$$

The poles of the observer resulted to be faster than the closed loop poles. This observer will be used in all the following LQ schemes with no alterations.

LQ1

The first controller aims to reproduce a classic control law used with the LQ. As written in (9) it is suggested to choose the matrix Q in order to punish the generator speed integral state and the angle velocity of the platform. The angle velocity of the tower has been punished following the same criteria. It has been considered the Bryson's Rule for the second and third element of Q, that are chosen considering that the controller objective is to limit the variations in generator speed at 49 rad/sec and the drivetrain torsion to 0.05 rad. The remaining weights are chosen by a "trial-and-error" procedure so as to have better performance of the closed loop system with respect to the baseline controller.

$$Q = diag([0, \frac{1}{(0.05)^2}, \frac{1}{49^2}, 0, 0, 10^8, 10^8, 0, 0, 10^3])$$

$$R = 10^6$$

$$N = [0 \quad 0 \quad 0 \quad 0 \quad 0 \quad 50 \quad 0 \quad 0]^T$$

The matrix N aims to limit the pitch rate of the actuator, as described in Appendix A. An integral action has been added in order to maintain the generator speed at the rated value. This solution has also been adopted for the other two LQ controllers.

Starting from these matrixes it is possible with the $lqr(A, B, Q, R, N)$ function in MATLAB to compute the K gain, that must be multiplied by the estimated state.

LQ2

In this controller it has been applied a minimization of the variance of $(\gamma - \alpha)$, that models the deflection of the tower. This minimization has been made considering the fatigue of the tower. In fact, it has been thought that minimizing the variance of the tower deflection, the fatigue of the tower base could decrease too. The R and N matrixes are kept equal to the LQ1, while the Q matrix is changed. Besides, only the weights concerning the tower and platform are changed, in order to be able to compare the results of the controllers. The Q matrix is then:

$$Q = \begin{bmatrix} 0 & & & & & & & & & \\ & \frac{1}{(0.05)^2} & & & & & & & & \\ & & \frac{1}{49^2} & & & & & & & \\ & & & 10^8 & -10^8 & & & & & \\ & & & -10^8 & 10^8 & & & & & \\ & & & & & 0 & & & & \\ & & & & & & 0 & & & \\ & & & & & & & 0 & & \\ & & & & & & & & 0 & \\ & & & & & & & & & 10^3 \end{bmatrix}$$

The explanation of this Q matrix is presented in the Appendix A. Here it is important to note that it allows to reduce the standard deviation of the tower deflection.

LQ3

The last controller is made considering another interpretation of the fatigue model used. As explained above, the fatigue is considered dependent primarily by the number of zero-crossing of the specified output. This means that the standard deviation could not be a good index for minimizing the fatigue. It should be smarter to reduce the variance of the derivative of $(\gamma - \alpha)$. In fact, the variance minimized in the LQ2 was given by:

$$var(\gamma - \alpha) = \int_{-\infty}^{\infty} \Gamma_{\gamma-\alpha}(\omega) d\omega \qquad (2.24)$$

While the variance of $\dot{\gamma} - \dot{\alpha}$ is:

$$var(\dot{\gamma} - \dot{\alpha}) = \int_{-\infty}^{\infty} \omega^2 \Gamma_{\gamma-\alpha}(\omega) d\omega \qquad (2.25)$$

By minimizing this variance it is possible to decrease the high frequency component of the tower deflection, that is what actually most affects the fatigue of the tower base loads. The Q matrix is almost the same as before, but the weight is moved on $\dot{\gamma} - \dot{\alpha}$, as follows:

$$Q = \begin{bmatrix} 0 & & & & & & & & & & \\ & \frac{1}{(0.05)^2} & & & & & & & & & \\ & & \frac{1}{49^2} & & & & & & & & \\ & & & 0 & 0 & & & & & & \\ & & & 0 & 0 & & & & & & \\ & & & & & 10^8 & -10^8 & & & & \\ & & & & & -10^8 & 10^8 & & & & \\ & & & & & & & 0 & & & \\ & & & & & & & & 0 & & \\ & & & & & & & & & 10^3 & \end{bmatrix}$$

Again, R and N are the same used in LQ1.

2.4.3 FAST

Simulations of the explained control systems are made with FAST (Fatigue, Aerodynamics, Structures and Turbulence) Code (1). FAST can model the dynamic response of different types of wind turbine, among which there also is the ballast stabilized floating wind turbine. The model used consist of a combined modal and multi-body dynamics formulation. A combination of rigid (platform, nacelle, armature, gears, hub) and flexible (tower, blades, driveshaft) bodies has been used to model the behavior of the wind turbine.

In a floating wind turbine 24 DOFs are used. Six DOFs are dedicated to the translational and rotational motion of the platform. Four DOFs account for the tower deflection: two are for the first and second bending moment of the fore-aft motion of the tower, and two are for the side-side motion. It is possible to use also a DOF for the yaw motion of the nacelle, that in this dissertation has not been considered, as part of

a different control loop. In order to model the drivetrain torsion two DOF are considered: one is for the azimuth angle of the rotor, and one accounts for the compliance between the hub and the generator. Six DOFs are used to describe the first and second flapwise mode of the blades, and three more are for the first edgewise mode. Finally two DOFs are used for the rotor and tail furl, that in this thesis are not considered.

Wind is given as an input in FAST and is computed by TurbSim (27), that is a stochastic turbulent wind simulator. Waves parameters are defined in one of the input file in FAST.

In this dissertation the specification of (10) have been used: starting from the data that Statoil used for their support platform in the Hywind Demo, Jonkman has developed a similar platform to support the 5-MW wind turbine, that is considered a standard wind turbine in NREL. This system is referred as "OC-3 Hywind", to distinguish it from the Statoil's implementation.

2.4.4 Experimental Setup

The control systems explained in this dissertation are compared in the same environmental conditions. Wind has a mean speed of 18 m/s, with turbulence intensity of 14.92% and air density 1.225 Kg/m^3. Waves are generated with an irregular spectrum, with a significant wave height of the incident waves of 6 m. Water density is 1025 Kg/m^3 and water depth is 320 m. The simulation time is 250 seconds.

The simulations were performed with FAST v7.01.00a-bjj and Aerodyn v13.00.01a-bjj compiled as S-Function in Simulink MATLAB (v7.14.0.739) with OC3 Hywind modifications on Windows 7 32 bit. DEL's analysis is performed using MCrunch v1.00 (28).

3 Results and Discussion

3.1 Performance Results

The electrical power output of the four presented controller are presented in Figure 3.1. The objective is to produce rated power (5 MW) minimizing its oscillations.

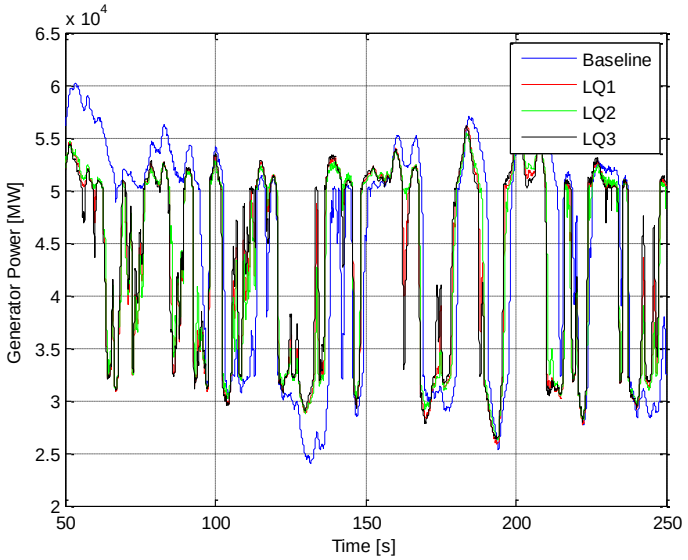

Figure 3.1 – Generated electric power time series. Blue is the realization with the baseline controller. Red, green and black are respectively with the LQ1, LQ2 and LQ3.

With the wind used for the simulations the generator speed is not always in Region 3, where there should be the rated power generation. Thus, the generator power is not close to the 5 MW. Besides, considering the constant torque control law in full-load region, it is interesting to look at the generator speed time-series of the four controllers.

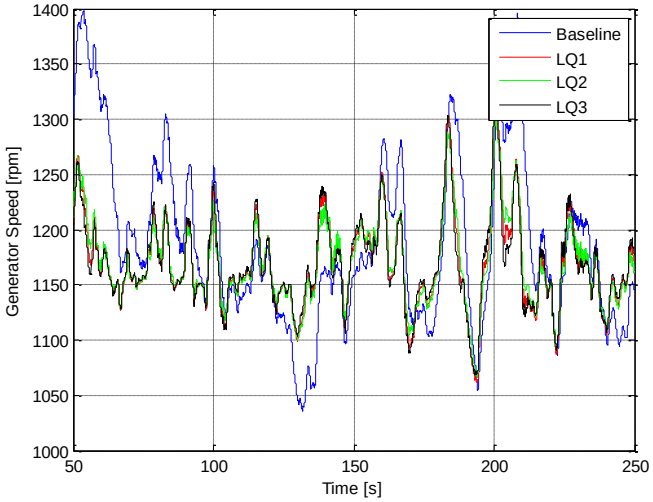

Figure 3.2 - Generator speed time series. Blue is the realization with the baseline controller. Red, green and black are respectively with the LQ1, LQ2 and LQ3.

In the Figure 3.2 the generator speed of the baseline showed to be the most changing between the four controllers. A statistics analysis can be useful in order to understand the behavior of the three controllers, as presented in Table 3.1:

Controller	Mean [rpm]	Standard Deviation
Baseline	1185	76.94
LQ1	1170	44.24
LQ2	1170	41.57
LQ3	1170	42.53

Table 3.1 – Mean and standard deviation of the generator speed for the baseline and the three LQ controllers.

The objective of this thesis is to reduce the fatigue in the tower base. It can be useful then to show the time-series of the tower deflection in the four controller's simulations, as done in Figure 3.3:

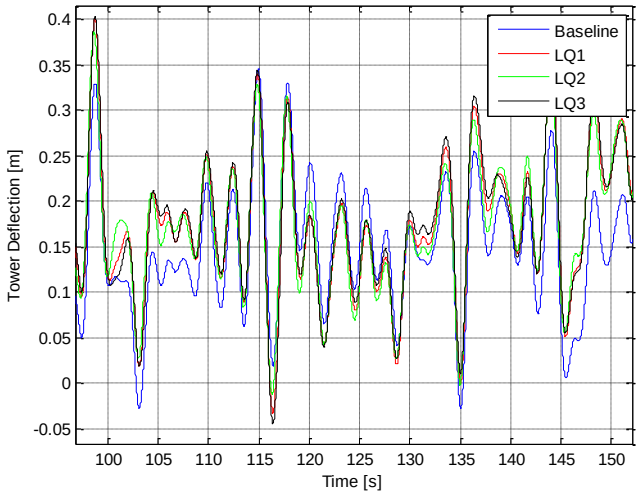

Figure 3.3 – Tower top deflection time series. Blue is the realization with the baseline controller. Red, green and black are respectively with the LQ1, LQ2 and LQ3.

Again, the statistical analysis can be helpful in order to discuss the performances of the controllers, as showed in Table 3.2:

Controller	Standard Deviation
Baseline	8.893E-02
LQ1	8.930E-02
LQ2	8.564E-02
LQ3	8.933E-02

Table 3.2 – Standard deviations of the tower deflection for the baseline and the three LQ controllers.

The mean value is not important in the case of the tower deflection, because not relevant for the fatigue computations.

The blade pitch actuator activity is showed in Figure 3.4:

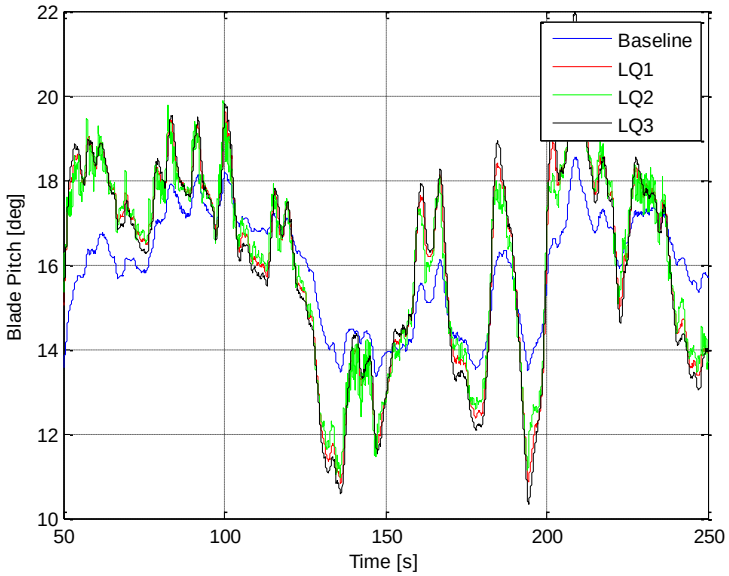

Figure 3.4 – Blade pitch angle time series. Blue is the realization with the baseline controller. Red, green and black are respectively with the LQ1, LQ2 and LQ3.

For the blade pitch actuator, instead of analyzing the pitch itself, the pitch rate has been analyzed. As presented Figure 3.4 in fact the blade pitch remains for all the controller inside reasonable limit, while it is important to understand if the pitch rates are increased too much with the LQ controllers. Finally, a Damage Equivalent Loads analysis is performed. The tower base loads, blade root loads and aerodynamic torque are used to compute the DELs.

The comparison is made in the Figure 3.5, where the statistical results are grouped with the DEL analysis. The performances of the generic index k are evaluated considering the equation (3.1):

$$k = \frac{k_{baseline} - k_{LQ,i}}{k_{baseline}} \qquad (3.1)$$

Thus, in the Figure 3.5 a positive value corresponds to better performances of the LQ regulator compared to the baseline controller.

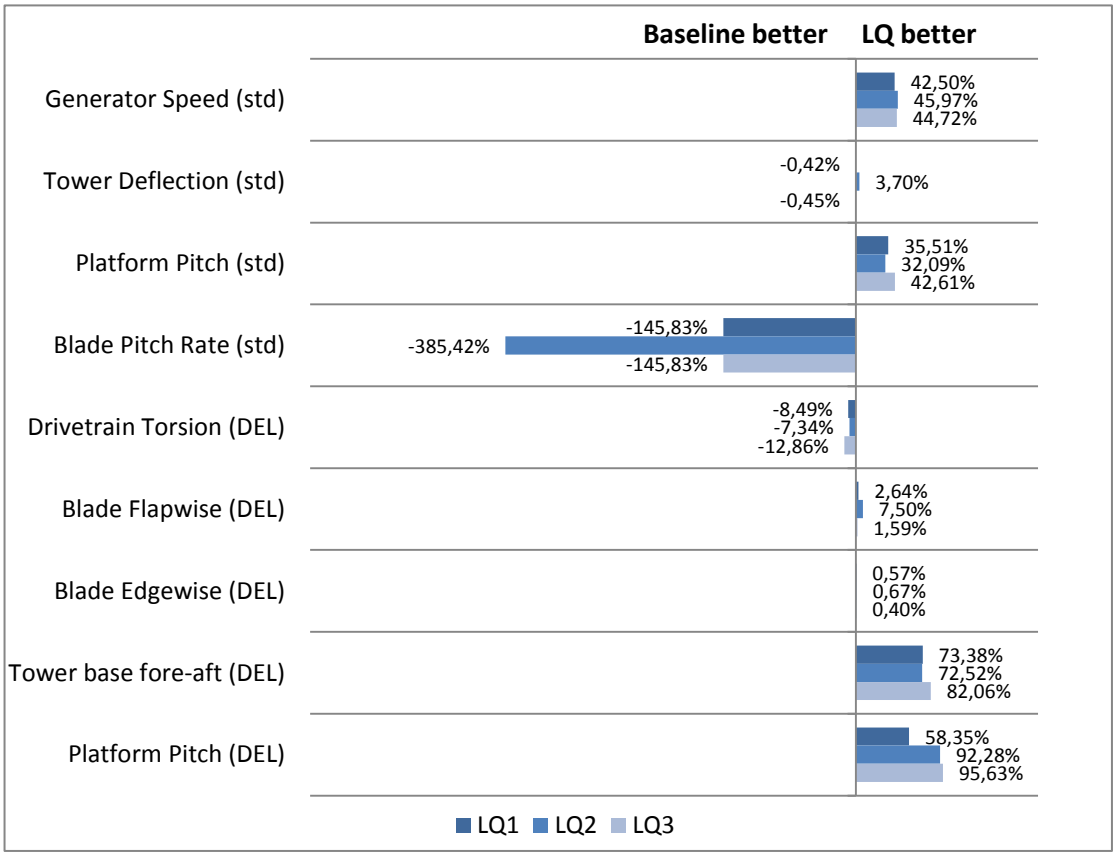

Figure 3.5 – Statistical and DELs analysis of LQ1, LQ2 and LQ3 compared to the baseline controller. A positive value means better performances of the LQ controller.

3.2 Discussion

The discussion is made following the results showed above, in which the generator speed regulation and DELs are evaluated. The generated electrical power cannot be compared considering the rated power of 5 MW because the variable speed regulator is not always in full load region. Besides, a constant torque approach is used, then an evaluation of the generator speed regulation is enough for describing the behavior of the controller. As showed in Figure 3.5 all the three LQ controllers have a better generator speed regulation. In Table 3.1 the mean and standard deviation of the generator speed are showed. Considering the rated generator speed equal to 1173.7 rpm, the baseline controller presents a mean over speed of 11.3 rpm, while in the LQ controllers there is a down speed of 3.7 rpm. The standard deviations of the LQ controllers are actually decreased of a factor of almost 40%. There are slight differences between the LQ1 and the other two, where the objectives are to decrease specifically the variance of the tower deflection, or of the tower deflection velocity. The use of different objectives could have given to the regulator the opportunity to increase the control action on the generator speed. In Table 3.2 the standard deviations of the tower deflection are presented for the controllers. The baseline, the LQ1 and LQ3 presented almost the same std. The LQ2 showed improvement in the standard deviation of the tower deflection of 3.7%: this is due to the objective of the

LQ2, that was actually to reduce the variance of the tower deflection. Besides, the decreased standard deviation evidenced that the fatigue of the tower base is not strictly connected to the variance of the deflection, while it is more dependent by the tower deflection rate. As explained above, this is due to the fatigue formulation, in which higher fatigue corresponds to higher number of cycles. Reducing the tower deflection rate in fact showed to be a good way to decrease the fatigue of the tower. In Figure 3.5 fatigue is more reduced when the LQ1 and LQ3 are used. Besides, also the LQ2 reduced the fatigue of a 72.52% compared to the baseline controller. The LQ3 showed the best results, with a 80.06% of fatigue reduction. The platform loads decreases significantly with the LQ controllers. Precisely, with the minimization of the variance of the tower deflection (LQ2), or tower deflection rate (LQ3), an improvement of almost 90% is presented. This might be due to the reduction of the tower deflection, that has an impact on the platform loads. A slight improvement of the blade flapwise fatigue is showed for the LQ controllers. This might be dependent by a lower platform pitch motion combined with the reduction of the tower deflection. The blade flapwise DELs didn't showed any improvement in performance. In fact, even though there is a reduction in the tower and platform motion, the augmented pitch activity induces blade flapwise loads.

The cost of these improvements is an incremented pitch actuator activity of 145,83% for the LQ1 and LQ3 and of 385% for the LQ2. Besides, the same pitch activity both for LQ1 and LQ3 showed that the use of a minimization of the tower deflection rate does not increase the pitch activity compared to others LQ objectives.

Also, the fatigue in the drivetrain torsion increased in all the LQ controllers. The LQ3 in particular increased the drivetrain fatigue of 12.86% compared to the baseline controller. This might be due to the increased pitch activity, that induces a more variable aerodynamic torque on the rotor, and of course more torsion considering that a constant torque approach is used for the generator. While in the baseline it has been suggested to use a constant torque approach, in the LQ a constant power can be a solution for decreasing also the fatigue of other components, where the torque can be used as control input in Region 3.

3.3 Conclusion

A model of floating wind turbine oriented to the description of the tower deflection, in addition to the platform pitch motion and drivetrain flexibilities, has been derived and validated. Three linear quadratic regulators based on this model have been applied with the high fidelity simulation software FAST, using an estimator for computing the unknown states starting from the available measures of the generator speed and tower deflection. Finally, a statistical and DELs analysis is made from the simulation results.

The results showed that the three LQ controllers achieved better performances in regulating the generator speed and decreasing the fatigue of the tower, at cost of an increased blade pitch activity and an acceptable increase of drivetrain torsion.

Anyhow, the two controllers that minimized the angle velocities (LQ1 and LQ3) of the tower and the platform, instead of the angle (LQ2), presented better performances in reducing the tower fatigue. Finally, a comparison between the LQ1 and LQ3 made clear that a control law that aims to reduce the tower deflection rate instead of the angles of the platform and tower is more effective in reducing the tower and platform fatigue. In fact, the results showed an improvement of 8.68% in the DEL of the tower base load, and of 37.28% in the platform loads.

References

1. **Jonkman, Bull.** FAST User's Guide. s.l. : National Renewable Energy Laboratory, 2005.

2. **Price, Trevor J.** Blyth, James (1839–1906). s.l. : Oxford Dictionary of National Biography (online ed.). Oxford University Press. doi:10.1093/ref:odnb/100957, 2004.

3. **EWEA.** EWEA - European Statistics Archive. [Online] 2012. http://www.ewea.org/statistics/european/.

4. **Shikha, Bhatti, T. S., Kothari, D. P.** Aspects of technological development of wind turbines, 129. 2003.

5. **T. Burton, N. Jenkins, D. Sharpe, E. Bossanyi.** Wind Energy Handbook (Second Edition). s.l. : Wiley and Sons, 2011. ISBN 978-0-470-69975-1.

6. **Christiansen, Søren.** Model–Based Control of a Ballast–Stabilized Floating Wind Turbine Exposed to Wind and Waves. s.l. : PhD Thesis, Aalborg University, 2013.

7. **G. Botta, E. Lembo and L. Serri.** Studio preliminare del comportamento dinamico di un aerogeneratore off-shore su supporto galleggiante. 2006. Rapporto CESI Ricerca 08000990.

8. **S. Butterfield, W. Musial, J. Jonkman, P. Sclavunos and , L. Wayman.** Engineering challenges for floating offshore wind turbines. s.l. : Golden, CO: National Renewable Energy Laboratory. NREL/CP-500-38776.

9. **S. Christiansen, T. Knudsen and T. Bak.** Optimal Control of a Ballast-Stabilized Floating Wind Turbine. s.l. : IEEE International Symposium on Computer-Aided Control System Design (CACSD), 2011.

10. **Jonkman, J.** Definition of the Floating System for Phase IV of OC3. 2010. NREL/TP-500-47535.

11. **Statoil.** Hywind - The world's full scale floating wind turbine. [Online] 2013. http://www.statoil.com/en/technologyinnovation/newenergy/renewablepowerproduction/offshore/hywind/pages/hywindputtingwindpowertothetest.aspx.

12. **Sclavounos, J. Jonkman and P.** Development of fully coupled aeroelastic and hydrodynamic models for offshore wind turbines. s.l. : NREL, 2006.

13. **Jonkman, J.** Dynamics Modeling and Loads Analysis of an Offshore FloatingWind Turbine. s.l. : PhD NREL, 2007.

14. **Skaare, Nielsen, Hanson.** Integrated Dynamic Analysis of Floating Offshore Wind Turbines. s.l. : Hydro Oil & Energy, 2007.

15. **Skaare, Hanson and Nielsen.** Importance of control strategies on fatigue life of floating wind turbines. 2007. Proceedings of 26th International Conference on Offshore Mechanics and Arctic Engineering.

16. **Hanson, T.J. Larsen and T. D.** A method to avoid negative damped low frequent tower vibrations for a floating, pitch controlled wind turbine. 2007. Journal of Physics: Conference Series 75 012073.

17. **Jonkman, J.** Influence of Control on the Pitch Damping of a Floating Wind Turbine. s.l. : NREL, 2008. NREL/CP-500-42589.

18. **Stol, Namik and.** State-Space control of tower motion for deepwater floating offshore wind turbines. s.l. : 76th AIAA Aerospace Sciences Meeting and Exhibit, 2008. AIAA 2008-1307.

19. **Lackner, Matthew A.** Controlling Platform Motions and Reducing Blade Loads for Floating Wind Turbines. 2009. Wind Engineering Volume 33, No. 6, pp. 541–553.

20. **Namik, Stol.** Control Methods for Reducing Platform Pitching Motion of Floating Wind Turbines. s.l. : Department of Mechanical Engineering, The University of Auckland, Auckland, New Zealand, 2009.

21. **s. Christiansen, T. Bak and T. Knudsen.** Minimum Thrust Load Control for Floating Wind Turbine. 2012. IEEE International Conference on Control Applications (CCA).

22. **Søren Christiansen, Thomas Bak and Torben Knudsen.** Damping Wind and Wave Loads on a FloatingWind Turbine. 2013. Vol. Energies, ISSN 1996-1073.

23. **G. Betti, M. Farina, A. Marzorati and R. Scattolini.** Platform, Modeling and Control of a Floating Wind Turbine with Spar Buoy. 2012. Vol. 2nd IEEE ENERGYCON Conference & Exhibition.

24. **Downing, S. D. and Socie, D. F.** Simple rainflow counting algorithms. s.l. : International Journal of Fatigue, 4:31–40, 1982.

25. **A. D. Wright, L. J. Fingersh.** Advanced Control Design for Wind Turbines, Part I. s.l. : NREL/TP-500-42437, 2008.

26. **J. Jonkman, S. Butterfield, W. Musial, and G. Scott.** Definition of a 5-MW Reference Wind Turbine for Offshore System Development. s.l. : NREL/TP-500-38060, 2009.

27. **B.J. Jonkman, L. Kilcher.** TurbSim User's Guide. s.l. : NREL/TP-xxx-xxxx, 2012.

28. **M. Buhl, Jr.** MCrunch User’s Guide. 2008. Vol. NREL/TP-500-43139 .

29. **Hansen, M. H., Hansen, A., Larsen, T. J., Фуе, S., Sørensen, and Fuglsang, P.** Control Design for a Pitch-Regulated, Variable-Speed Wind Turbine. s.l. : Risø-R-1500(EN), Roskilde, Denmark: Risø National Laboratory, 2005.

Appendix A

A.1 LQ Control in a Wind Turbine

The LQ regulator is designed over a linear state-space model of the wind turbine represented by the matrixes A, B, C and D:

$$\begin{cases} \dot{x} = Ax + Bu \\ y = Cx + Du \end{cases}$$

where $\overline{x} \in R^N$ is the state vector, $\overline{u} \in R^M$ is the control input vector and $\overline{y} \in R^P$ is the measured output vector. The matrix A represent the state matrix, B the control gain matrix and C relates the measured output with the turbine states. Usually for a wind turbine it is possible to consider $D = 0$. In order to apply the LQ theory the system as to be controllable. To check the controllability the following theorem can be used:

***THEOREM**: the system (A,B) is controllable if and only if* $rank[B: AB: A^2B: \dots]$ *is equal to N.*

The LQ controller uses the control law:

$$u = -Kx$$

where K is the gain the minimizes the cost function J:

$$J = \int_0^\infty (\overline{x}^T Q\overline{x} + \overline{u}^T R\overline{u} + 2\overline{x}^T N\overline{u})dt$$

where Q(N,N) is symmetric, positive semidefinite, and it weights the state vector, and R(M,M) is symmetric, positive definite, and weights the input vector. N(N,M) is a cross weight between the state and the input vector. The state-feedback gain is computed from the solution S of the associated Riccati equation:

$$A^TS + SA - (SB + N)R^{-1}(B^TS + N^T) + Q = 0$$

The control gain is then:

$$K = R^{-1}(B^TS + N^T)$$

In this thesis it has been used the function $lqr(A, B, Q, R, N)$ in MATLAB, that gives as an output the vector K and the solution S of the Riccati equation.

Integral State on the Generator Speed

The main purpose of a wind turbine controller is to regulate the generator speed at rated value. In order to do so an integral state for the generator speed can be added. The state vector will have one more state as follows:

$$\dot{x}_{10} = \omega$$

Where ω is the generator speed. In this way it is possible to add an integral action, and the generator speed is regulated to have an error equal to zero.

Actuator pitch rate limiting

One way of limit the actuator blade pitch rate is to use the matrix N. In fact, the dynamics of β in the state space model is:

$$\dot{\beta} = \frac{1}{\tau_\beta}(\beta_c - \beta)$$

where β is a state of the system and β_c is a control input. Considering as zero all the elements of Q and N except for Q(8,8)=1 and N(1,8)=1, and imposing R=1 the cost function J can be computed as follows

$$J = \beta^2 + \beta_c^2 - 2\beta\beta_c = (\beta_c - \beta)^2$$

So J represent the variance of dynamics of the actuator, and minimizing it means to minimize the actuator pitch rate.

LQ2 – LQ3

In order to minimize the variance of the $\gamma - \alpha$ it has been used in the elements (4:5,4:5) of Q the sub-matrix:

$$Q(4{:}5,4{:}5) = \begin{bmatrix} q_{\gamma\alpha} & -q_{\gamma\alpha} \\ -q_{\gamma\alpha} & q_{\gamma\alpha} \end{bmatrix}$$

In fact, solving the cost function J considering as 0 all the other element of Q, R and N, J would be:

$$J = \alpha^2 q_{\gamma\alpha} - \gamma\alpha q_{\gamma\alpha} - \gamma\alpha q_{\gamma\alpha} + \gamma^2 q_{\gamma\alpha} = q_{\gamma\alpha}(\gamma - \alpha)^2$$

In the LQ3 it is used the same approach, but moving the sub-matrix in the element (6:7,6:7) of Q, so as to weight the $\dot{\gamma} - \dot{\alpha}$.

State Estimator

The state-estimator is based on a Kalman filter. The system, to be estimate, must be observable. The observability can be checked with the following:

***THEOREM**: a system (A,C) is observable if and only if* $rank[C; CA; CA^2; \dots] = N$

The estimator can be computed choosing a matrix Q_{obs} and R_{obs} for the observer. The state observer is described by the equation:

$$\dot{\hat{x}} = A\dot{\hat{x}} + Bu + L(y - C\dot{\hat{x}})$$

where $\dot{\hat{x}}$ is the state estimation. Again, the vector L is computed from the solution of the Riccati equation. In MATLAB can be used the same function giving as an input the matrixes as follows:

$$lqr(A^T, C^T, Q_{obs}, R_{obs})$$